Обзор ArXiv:astro-ph , 4-8 декабря 2017 года

От Сильченко О.К.

Astro-ph: 1712.01283

SPATIALLY RESOLVED KINEMATICS IN THE CENTRAL 1 KPC OF A COMPACT STAR-FORMING GALAXY AT $z \sim 2.3$ FROM ALMA CO OBSERVATIONS

G. Barro[1,2] M. Kriek[2], P. G. Pérez-González[3] T. Diaz-Santos[4], S. H. Price[5], W. Rujopakarn[6,7,8], V. Pandya[9], D. C. Koo[9], S. M. Faber[9], A. Dekel[10], J. R. Primack[11], D. D. Kocevski[12]

Last edited: December 6, 2017

ABSTRACT

We present high spatial resolution (FWHM$\sim$0.″14) observations of the CO$(8-7)$ line in GDS-14876, a compact star-forming galaxy at $z = 2.3$ with total stellar mass of $\log(M_\star/M_\odot) = 10.9$. The spatially resolved velocity map of the inner $r \lesssim 1$ kpc reveals a continous velocity gradient consistent with the kinematics of a rotating disk with $v_{\rm rot}(r = 1{\rm kpc}) = 163 \pm 5$ km s^{-1} and $v_{\rm rot}/\sigma \sim 2.5$. The gas-to-stellar ratios estimated from CO$(8-7)$ and the dust continuum emission span a broad range, $f_{\rm gas}^{\rm CO} = M_{\rm gas}/M_\star = 13-45\%$ and $f_{\rm gas}^{\rm cont} = 50-67\%$, but are nonetheless consistent given the uncertainties in the conversion factors. The dynamical modeling yields a dynamical mass of $\log(M_{\rm dyn}/M_\odot) = 10.58^{+0.5}_{-0.2}$ which is lower, but still consistent with the baryonic mass, $\log(M_{\rm bar}=M_\star + M_{\rm gas}^{\rm CO}/M_\odot) = 11.0$, if the smallest CO-based gas fraction is assumed. Despite a low, overall gas fraction, the small physical extent of the dense, star-forming gas probed by CO$(8-7)$, $\sim 3\times$ smaller than the stellar size, implies a strong relative concentration that increases the gas fraction up to $f_{\rm gas}^{\rm CO,1kpc} \sim 85\%$ in the central 1 kpc. Such a gas-rich center, coupled with a high star-formation rate, SFR$\sim$ 500 M$_\odot$ yr^{-1}, suggests that GDS-14876 is quickly assembling a dense stellar component (*bulge*) in a strong nuclear starburst. Assuming its gas reservoir is depleted without replenishment, GDS-14876 will quickly ($t_{\rm depl} \sim 27$ Myr) become a compact quiescent galaxy that could retain some fraction of the observed rotational support.

GDS-14876: повышенный темп SF, но компактность, как у пассивных

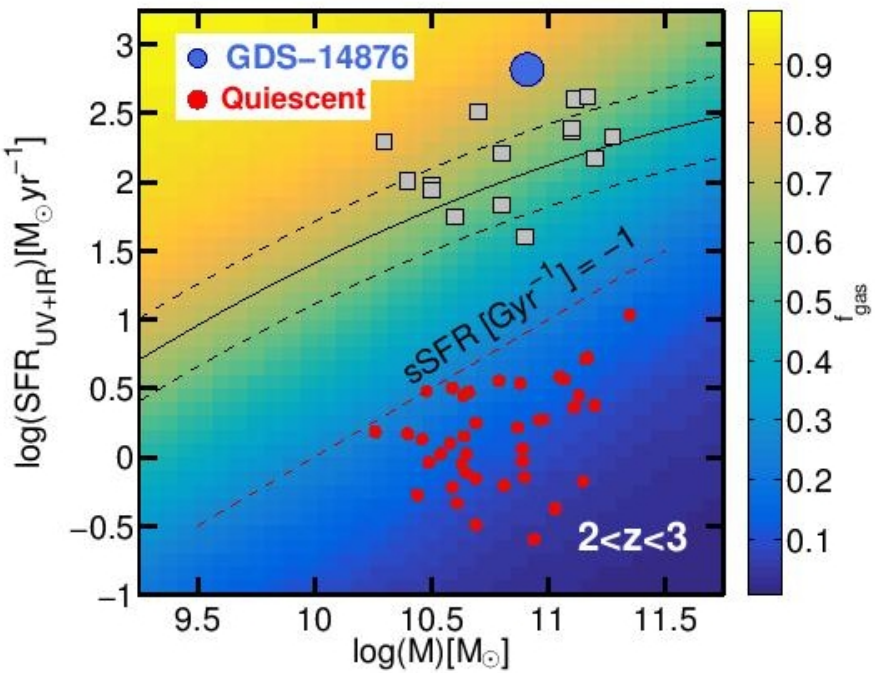

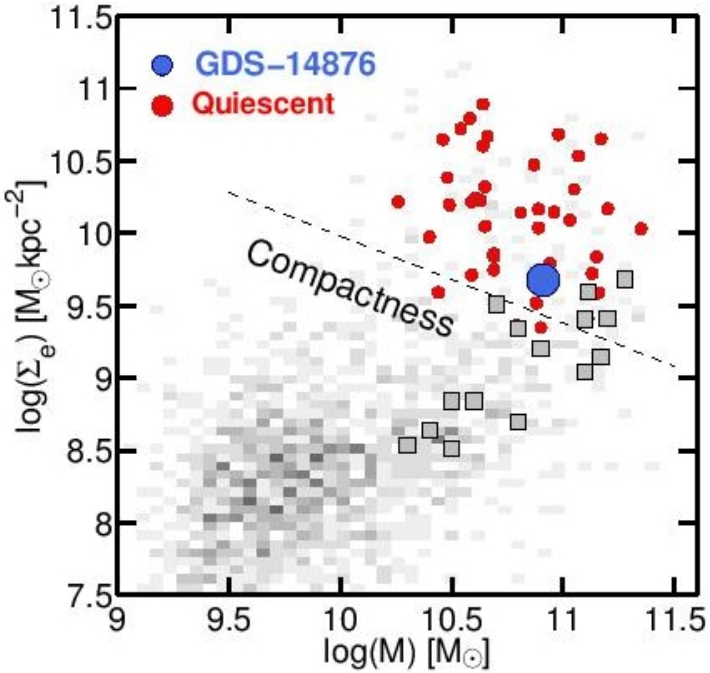

FIG. 1.— *Left:* Logarithm of SFR vs. stellar mass for GDS-14876 (blue circle) and other massive SFGs at $z \sim 2$ (grey squares) observed with ALMA and HST, drawn from Spilker et al. (2016), Rujopakarn et al. (2016) and Popping et al. (2017). The black lines show the locus and ×5 limits (solid and dashed) of the SFR sequence at $z = 2.25$ from Whitaker et al. (2014). The background is colored by the predicted gas fraction determined from the empirical prediction of Genzel et al. (2015). GDS-14876 lies above the SFR sequence and is expected to have a large $f_{gas} \sim 80\%$. The red line and circles show the location of the quiescent population at the same redshift, selected by low sSFR< -1 Gyr^{-1}. *Right:* Logarithm of the effective mass surface density vs. stellar mass for galaxies in CANDELS-GDS at $z \sim 2$ (greyscale) and all galaxies from the left panel. The dashed line indicates the *compactness* selection criterion of Barro et al. (2017).

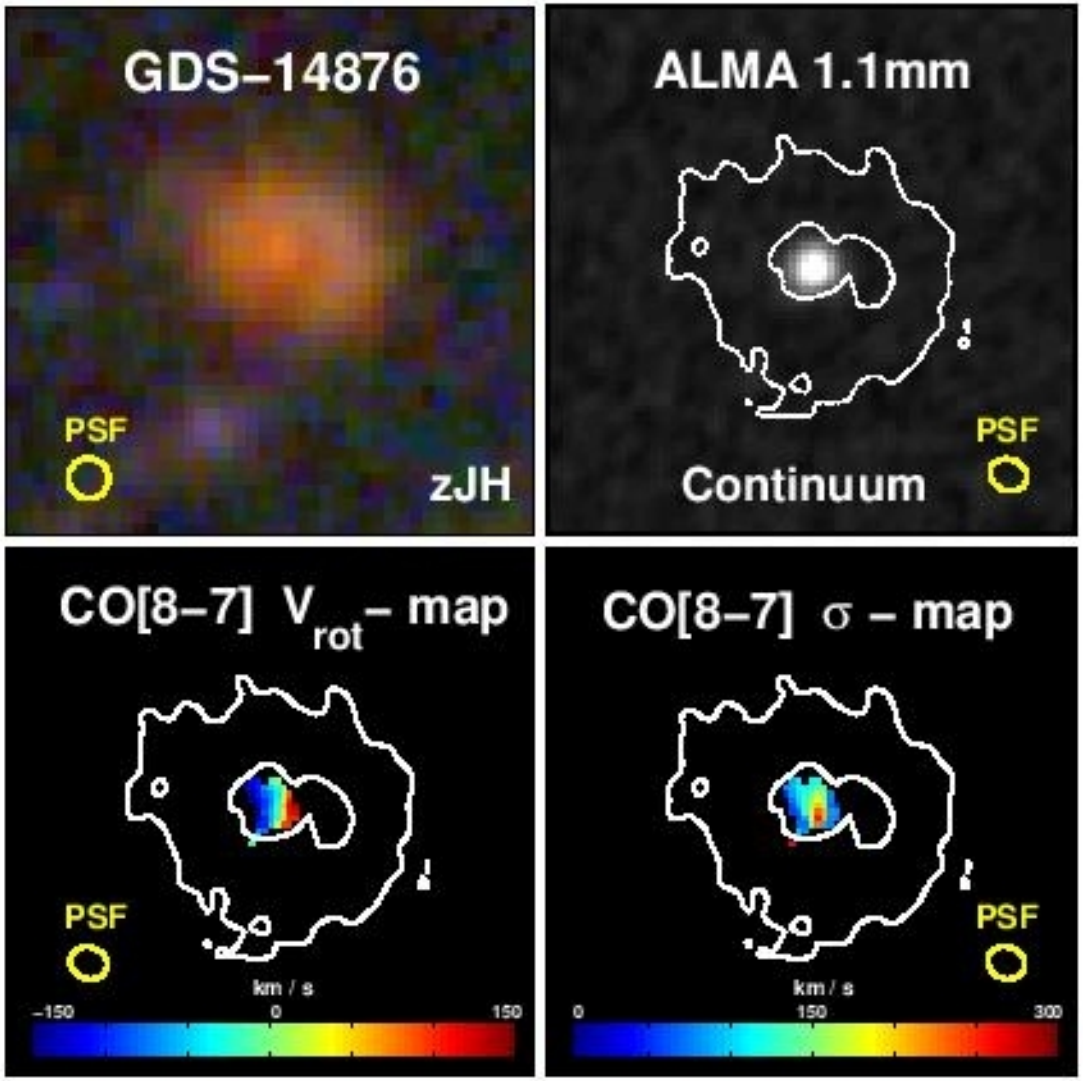

FIG. 2.— *Left:* From top to bottom, $2''.5 \times 2''.5$ (20×20 kpc) images

Кривая вращения соответствует гравитации звездного диска

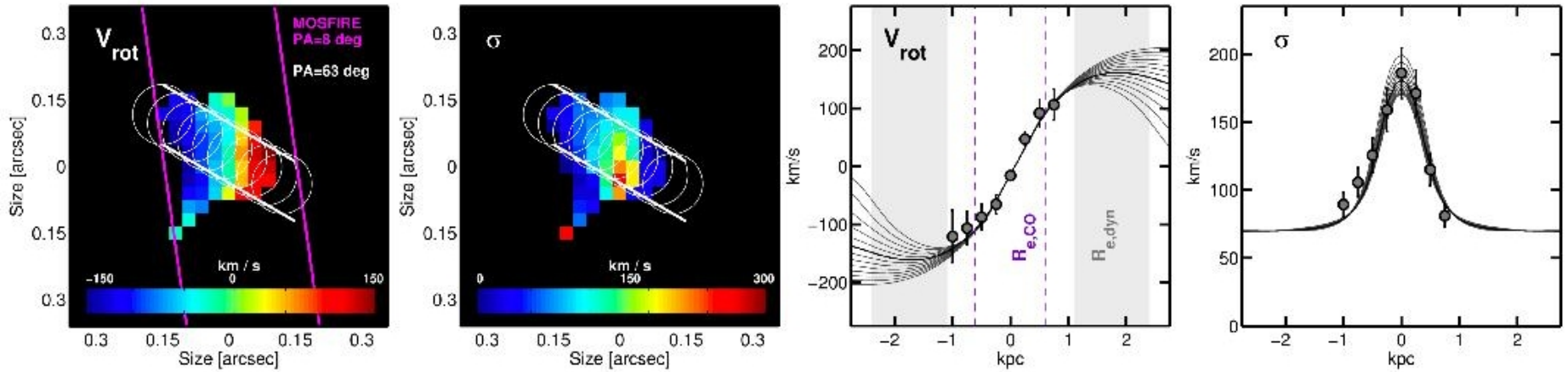

FIG. 4.— *Left:* Moment maps of the central region of GDS-14876 showing the projected CO velocity field and velocity dispersion where S/N$\geq$ 3. The white circles marking the extracted pseudo slit using apertures with the FWHM of the minimum resolution element. The magenta lines illustrate the orientation of the slit in the MOSFIRE [OIII] observations, which is misaligned with the CO kinematic major axis by $\sim 50°$. *Right:* Observed (grey circles) and best-fit models (black line and 1σ grey) for the rotation velocity and velocity dispersion profiles along the kinematic major axis. The dynamical modeling of the kinematic maps is consistent with a rotating disk of gas. The dashed lines and grey regions indicate the CO effective radius and the 1σ confidence for $r_e^{\rm dyn}$.

Быстрое (27 млн лет) формирование балджа

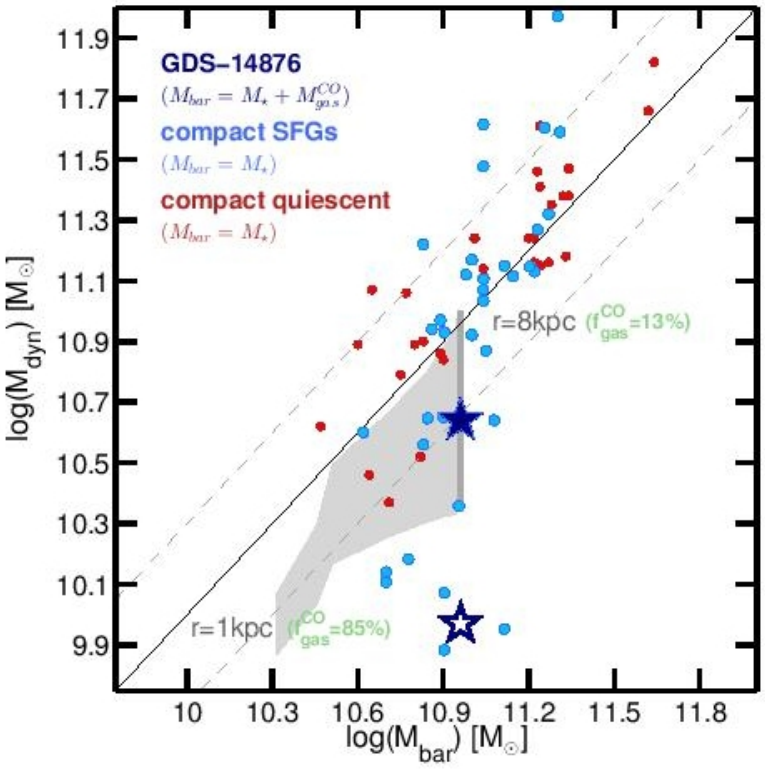

FIG. 5.— Comparison between the dynamical and stellar masses for GDS-14876 and other samples of compact SFGs (blue) and quiescent (red) galaxies from Barro et al. (2014b), van Dokkum et al. (2015), van de Sande et al. (2013) and Belli et al. (2014). The blue stars show M_{dyn} for GDS-14876 as computed from the CO (filled) and [OIII] (empty) lines. The grey shaded area depicts the confidence region of the comparison between cumulative M_{dyn} and $M_\star$with increasing radii from $r = 1$ kpc to $r = 8$ kpc

- Согласовать динамическую и барионную массу можно только в рамках гипотезы, что весь газ сосредоточен в центре (30% радиуса звездного диска).

Astro-ph: 1712.01860

An 800 million solar mass black hole in a significantly neutral universe at redshift 7.5

Eduardo Bañados[1,*], Bram P. Venemans[2], Chiara Mazzucchelli[2], Emanuele P. Farina[2], Fabian Walter[2], Feige Wang[3,4], Roberto Decarli[2,5], Daniel Stern[6], Xiaohui Fan[7], Fred Davies[8], Joseph F. Hennawi[8], Rob Simcoe[9], Monica L. Turner[9,10], Hans-Walter Rix[2], Jinyi Yang[3,4], Daniel D. Kelson[1], Gwen Rudie[1], and Jan Martin Winters[11]

[1]The Observatories of the Carnegie Institution for Science, 813 Santa Barbara St., Pasadena, CA 91101, USA
[2]Max Planck Institut für Astronomie, Königstuhl 17, D-69117, Heidelberg, Germany
[3]Department of Astronomy, School of Physics, Peking University, Beijing 100871, China
[4]Kavli Institute for Astronomy and Astrophysics, Peking University, Beijing 100871, China
[5]INAF – Osservatorio Astronomico di Bologna, via Gobetti 93/3, 40129, Bologna, Italy
[6]Jet Propulsion Laboratory, California Institute of Technology, 4800 Oak Grove Drive, Pasadena, CA 91109, USA
[7]Steward Observatory, The University of Arizona, 933 North Cherry Avenue, Tucson, AZ 85721–0065, USA
[8]Department of Physics, Broida Hall, University of California, Santa Barbara, CA 93106–9530, USA
[9]MIT-Kavli Center for Astrophysics and Space Research, 77 Massachusetts Avenue, Cambridge, MA, 02139, USA
[10]Las Cumbres Observatory, 6740 Cortona Dr, Goleta, CA 93117, USA
[11]Institut de Radioastronomie Millimétrique (IRAM), 300 rue de la Piscine, 38406 Saint Martin d'Hères, France
[*]ebanados@carnegiescience.edu

Обнаружение по фотометрии, и последующая спектроскопия на Магеллане

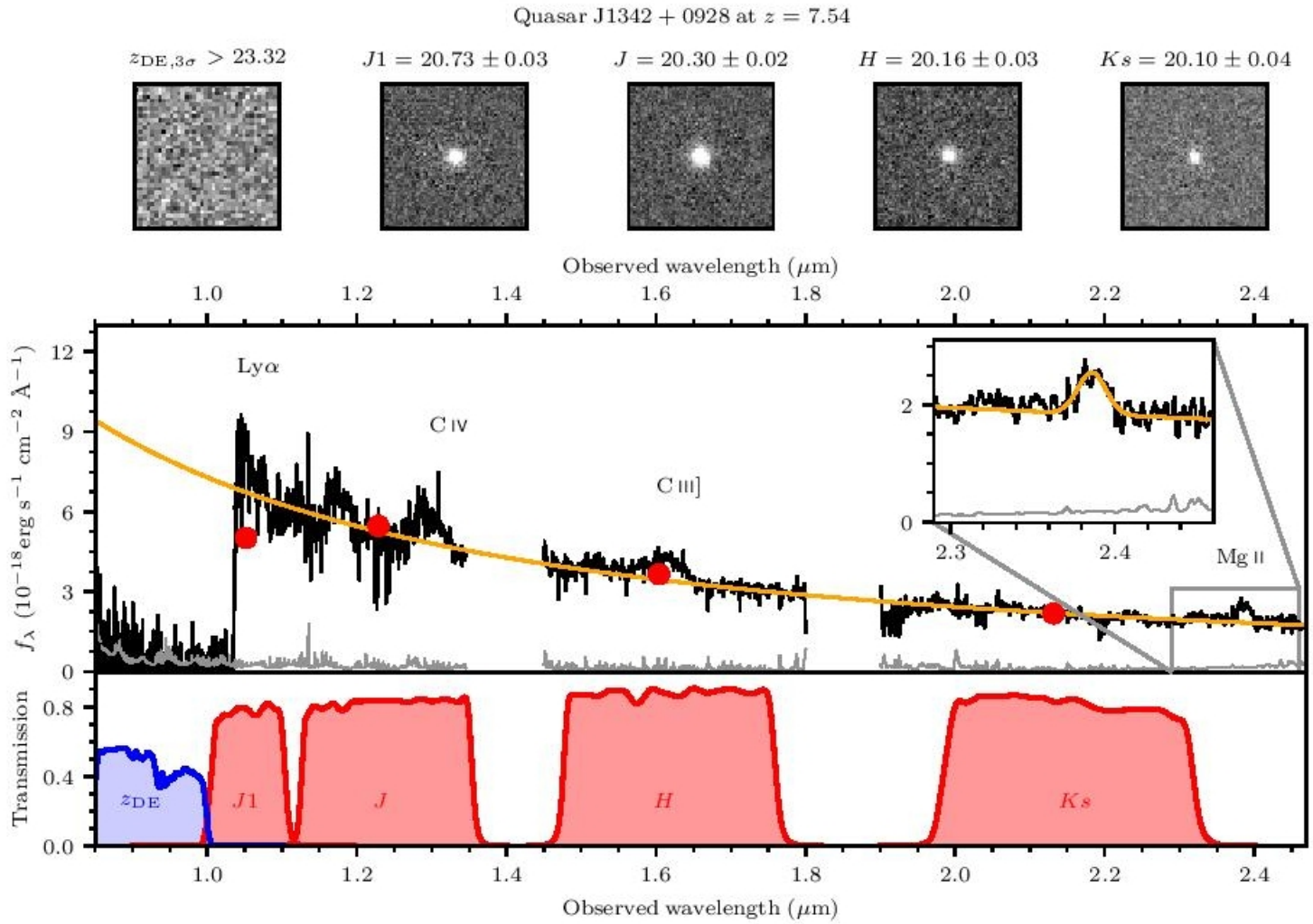

Модель: экспоненциальный рост черной дыры с z=40 из затравки в несколько 1000 масс Солнца

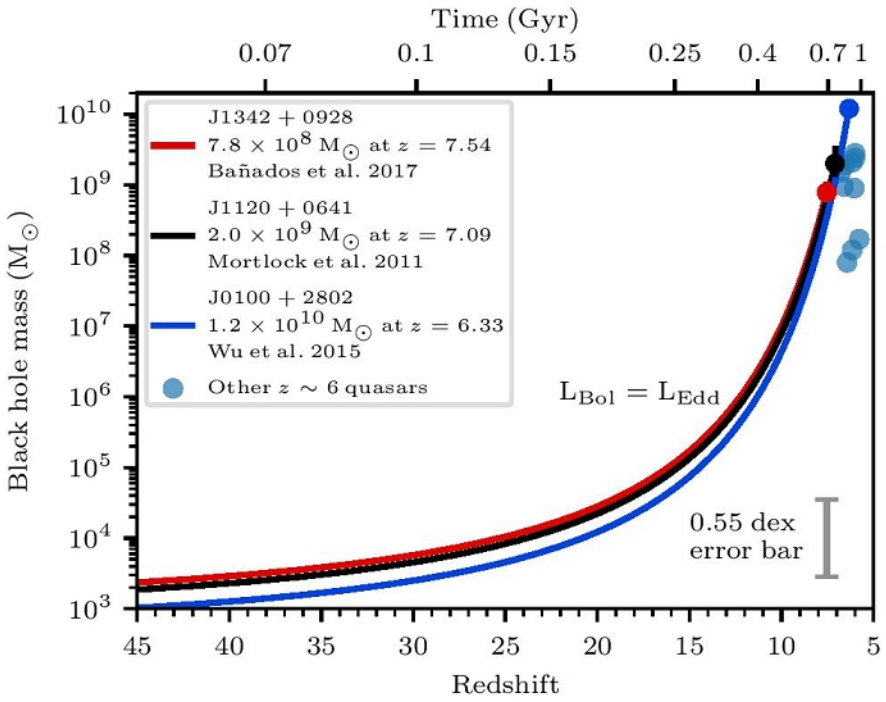

Figure 2. Black hole growth of three of the highest redshift and most massive quasars in the early universe, J1342+0928, J1120+0641[1], and J0100+2802[16]. The three curves are normalized to the observed black hole mass and redshift of these quasars (data points with statistical error bars). The black hole growth is modeled as $M_{BH} = M_{BH,seed} \times \exp(\text{time}/50\,\text{Myr})$, where we have assumed that the black holes are accreting at the Eddington limit ($L_{Bol} = L_{Edd}$) with a radiative efficiency of 10%. The circles show a compilation of black hole masses of $z \sim 6$ quasars[24]. The gray error bar at the bottom right represents dominant uncertainty due to systematics in the local

Astro-ph: 1712.01886

COPIOUS AMOUNTS OF DUST AND GAS IN A $Z = 7.5$ QUASAR HOST GALAXY

BRAM P. VENEMANS,[1] FABIAN WALTER,[1,2,3] ROBERTO DECARLI,[1,4] EDUARDO BAÑADOS,[5] CHRIS CARILLI,[3,6] JAN MARTIN WINTERS,[7] KARL SCHUSTER,[7] ELISABETE DA CUNHA,[8] XIAOHUI FAN,[9] EMANUELE PAOLO FARINA,[1] CHIARA MAZZUCCHELLI,[1] HANS-WALTER RIX,[1] AND AXEL WEISS[10]

[1]*Max-Planck Institute for Astronomy, Königstuhl 17, D-69117 Heidelberg, Germany*
[2]*Astronomy Department, California Institute of Technology, MC105-24, Pasadena, CA 91125, USA*
[3]*National Radio Astronomy Observatory, Pete V. Domenici Array Science Center, P.O. Box 0, Socorro, NM 87801, USA*
[4]*Osservatorio Astronomico di Bologna, via Gobetti 93/3, I-40129 Bologna, Italy*
[5]*The Observatories of the Carnegie Institution for Science, 813 Santa Barbara Street, Pasadena, CA 91101, USA*
[6]*Astrophysics Group, Cavendish Laboratory, JJ Thomson Avenue, Cambridge CB3 0HE, UK*
[7]*Institut de Radioastronomie Millimétrique (IRAM), 300 rue de la Piscine, F-38406 Saint Martin d'Hères, France*
[8]*Research School of Astronomy and Astrophysics, Australian National University, Canberra, ACT 2611, Australia*
[9]*Steward Observatory, The University of Arizona, 933 North Cherry Avenue, Tucson, AZ 85721-0065, USA*
[10]*Max-Planck-Institut für Radioastronomie, Auf dem Hügel 69, D-53121 Bonn, Germany*

(Received 2017 August 29; Revised 2017 October 13; Accepted 2017 October 17)

ABSTRACT

We present IRAM/NOEMA and JVLA observations of the quasar J1342+0928 at $z = 7.54$ and report detections of copious amounts of dust and [C II] emission in the interstellar medium (ISM) of its host galaxy. At this redshift, the age of the universe is

Свойства хозяйской галактики

Table 1. Observed and Derived Properties of J1342+0928

R.A. (J2000)	$13^h42^m08^s.097$
Decl. (J2000)	$+09°28'38''.28$
$z_{[CII]}$	7.5413±0.0007
$F_{[CII]}$ (Jy km s^{-1})	1.25±0.17
FWHM$_{[CII]}$ (km s^{-1})	383±56
EW$_{[CII]}$ (μm)	1.73±0.43
$S_{223.5\,GHz}$ (μJy)	415±73
$S_{135.5\,GHz}$ (μJy)	<139
$S_{95\,GHz}$ (μJy)	<48
$S_{41\,GHz}$ (μJy)	15.0±5.7
$S_{1.4\,GHz}$ (μJy)	<432
$F_{CO(3-2)}$ (Jy km s^{-1})	<0.081
$F_{CO(7-6)}$ (Jy km s^{-1})	<0.13
$F_{CO(10-9)}$ (Jy km s^{-1})	<0.32
$F_{[CI]}$ (Jy km s^{-1})	<0.14
$F_{H_2O,1172\,GHz}$ (Jy km s^{-1})	<0.30
$F_{H_2O,1918\,GHz}$ (Jy km s^{-1})	<0.33
L_{FIR} ($L_\odot$)	$(0.5-1.4)\times10^{12}$
L_{TIR} ($L_\odot$)	$(0.8-2.0)\times10^{12}$
$L_{[CII]}$ ($L_\odot$)	$(1.6\pm0.2)\times10^{9}$
$L_{[CI]}$ ($L_\odot$)	$<7.8\times10^{7}$
$L'_{CO(3-2)}$ (K km s^{-1} pc^2)	$<1.5\times10^{10}$
SFR$_{TIR}$ ($M_\odot$ yr^{-1})	120–300
SFR$_{[CII]}$ ($M_\odot$ yr^{-1})	85–545
M_d ($M_\odot$)	$(0.6-4.3)\times10^{8}$
M_{C+} ($M_\odot$)	4.9×10^{6}
M_{H_2} ($M_\odot$)	$<1.2\times10^{10}$

- Нет CO ни в каких переходах!
- Единственно измеряемые сигналы – в линии атомарного газа [CII]158 мкм и в континууме 41 ГГц
- Темпы звездообразования по [CII] и TIR – несколько сотен масс Солнца в год

Разные варианты модели SED по двум точкам

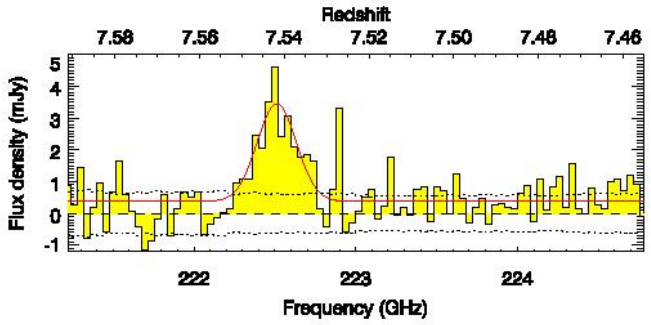

Figure 1. NOEMA spectrum of the redshifted [C II] emission line and the underlying continuum in J1342+092, extracted from the peak pixel in the datacube. The bin size is 40 MHz, which corresponds to $\sim$54 km s^{-1}. The dotted lines indicate $+\sigma$ and $-\sigma$, with σ being the noise in each bin. The red, solid line is a flat continuum plus Gaussian fit to the spectrum (the fit values are reported in Table 1).

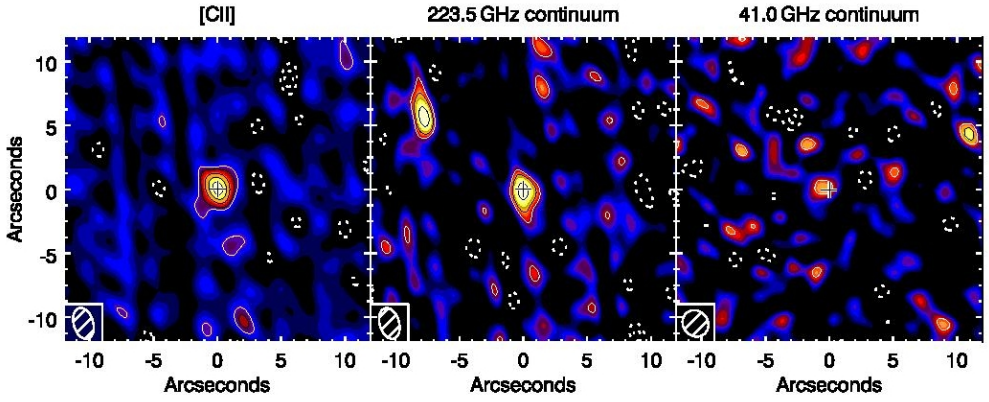

Figure 2. Maps of the [C II] emission (left), the continuum emission at 223.5 GHz (middle), and the continuum at 41.0 GHz of J1342+0928. The [C II] map was created by averaging the continuum-subtracted datacube over 455 km s^{-1} ($2.8 \times \sigma_{[CII]}$). The cross indicates the near-infrared position of the quasar. The beam is overplotted in the bottom left corner of each map. The contours show the emission at levels -3σ and -2σ (dotted lines) and $+2\sigma$, $+3\sigma$, $+5\sigma$, $+7\sigma$, and $+9\sigma$ (solid lines), where the σ denotes the noise in the image (247 μJy beam^{-1}, 73 μJy beam^{-1}, and 5.7 μJy beam^{-1}, respectively). The nearby millimeter continuum source (Section 2.1) can be seen toward the northeast in the middle panel.

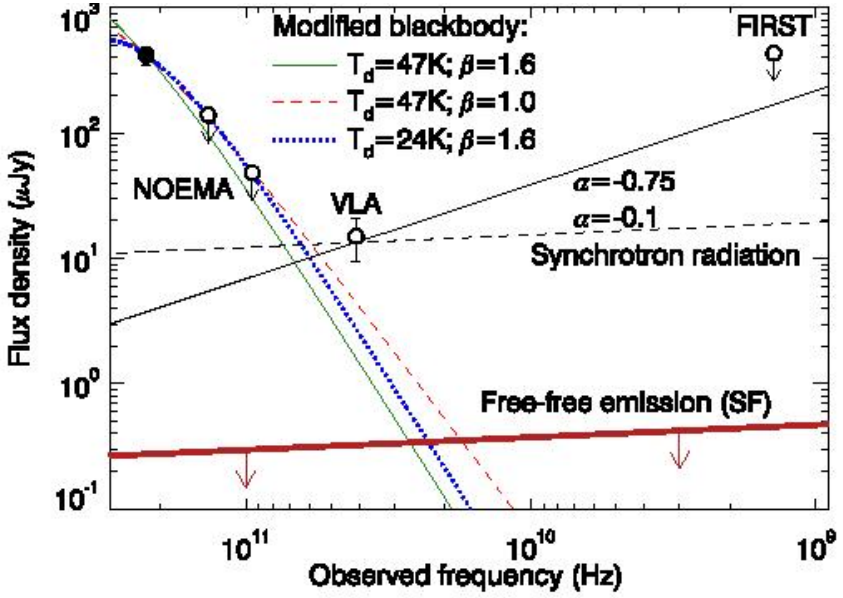

Figure 3. Far-infrared and radio spectral energy distribution of J1342+0928. The data points from left to right represent the NOEMA 1, 2, and 3 mm observations, the tentative VLA 41.0 GHz detection, and the FIRST upper limit. Overplotted are three different dust SEDs scaled to the 1 mm detection and two power laws describing radio synchrotron radiation. The dust model with canonical values ($T_d = 47$ K and $\beta = 1.6$) agrees well with the upper limits on the continuum emission at 2 and 3 mm, but predicts a much lower continuum flux density at 41.0 GHz. A shallower β ($\beta = 1.0$) or a lower dust temperature ($T_d = 24$ K, slightly above the CMB temperature at $z = 7.54$), illustrated by the dashed and dotted lines, also predicts a 41.0 GHz flux density below that of the tentative VLA source. The upper limit in FIRST does not provide strong constraints on the slope of the radio emission.

Сравнение масс галактики и черной дыры

3.5. *Dynamical mass estimate*

From the velocity dispersion σ of the [C II] emission and the radius R of the line emitting region, we can estimate a dynamical mass of the quasar host galaxy by utilizing the virial theorem: $M_{\rm dyn} = 3R\sigma^2/2G$ with G as the gravitational constant. Assuming that the velocity dispersion can be derived from the Gaussian fit to the [C II] emission (Figure 1), and adopting a maximum radius of the [C II] emission of $R < 3.5$ kpc (Section 3.3), we infer a dynamical mass $M_{\rm dyn} < 3.2 \times 10^{10}\,M_\odot$. If instead we assume that the [C II] emission is in a rotating disk with inclination angle i (e.g., Wang et al. 2013; Willott et al. 2015; Venemans et al. 2016), we derive a higher dynamical mass of $M_{\rm dyn} < 1.0 \times 10^{11}/\sin^2(i)\,M_\odot$. Adopting $i = 55°$, the median inclination angle of $z \sim 6$ quasar hosts (Wang et al. 2013), the dynamical mass of J1342+0928 becomes $M_{\rm dyn} < 1.5 \times 10^{11}\,M_\odot$, which is $\lesssim$190$\times$ higher that of the black hole (Bañados et al. 2017). To more accurately constrain the dynamical mass, high spatially resolved observations of the [C II] emission are necessary.

- Оценка динамической массы – по ширине линии [CII] и по верхнему пределу на радиус газового диска (он не разрешен в наблюдениях).

Astro-ph: 1712.02348

ON THE CGM FUNDAMENTAL PLANE: THE HALO MASS DEPENDENCY OF CIRCUMGALACTIC H I

RONGMON BORDOLOI[1,2], J. XAVIER PROCHASKA[3], JASON TUMLINSON[4,5], JESSICA K. WERK[6], TODD M. TRIPP[7], & JOSEPH N. BURCHETT[3]

Draft version December 8, 2017

ABSTRACT

We analyze the equivalent widths of H I Lyα ($W_{\rm Ly\alpha}$) from the inner ($R < 160$ kpc) circumgalactic medium (CGM) of 85 galaxies at $z \sim 0$ with stellar masses $M*$ ranging $8 \leq \log M*/M_\odot \leq 11.6$. Across three orders of magnitude in stellar mass, the CGM of present-day galaxies exhibits a very high covering fraction of cool hydrogen gas ($f_C = 86.6 \pm 3.6\%$) indicating that the CGM is ubiquitous in modern, isolated galaxies. These same galaxies show a decline in $W_{\rm Ly\alpha}$ with increasing radius, independent of mass, but the scatter in this trend correlates closely with $M*$. Using the radial and stellar mass correlations, we construct a fundamental plane describing the cool CGM of modern galaxies: $\log W^{\rm s}_{HI1215} = (0.34 \pm 0.02) - (0.0026 \pm 0.0005) * (R) + (0.286 \pm 0.002) * \log(M_*/M_\odot)$. The RMS scatter around this bivariate relation is $\sim$0.2 dex. We interpret the explicit correlation between $W_{\rm Ly\alpha}$ and $M*$ to arise from the underlying dark matter halo, i.e., $W_{\rm Ly\alpha}$ traces the gravitational potential whereas $M*$ tracks $M_{\rm halo}$.

Фактор покрытия – процент обнаруженных абсорбций среди наблюдавшихся

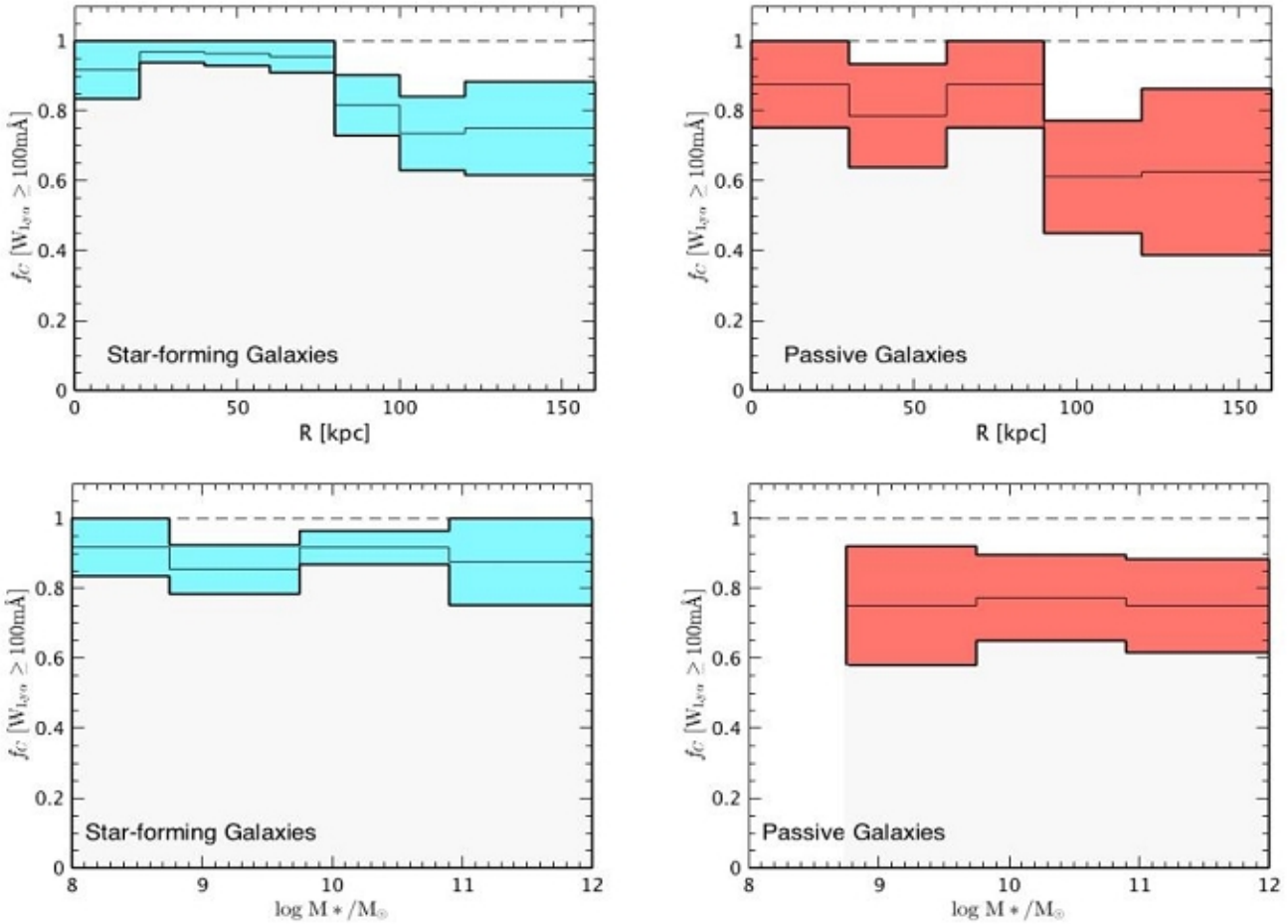

FIG. 1.— Covering fraction of Lyα absorption ($W_{Ly\alpha} \geq 100$ mÅ) as a function of observed impact parameter (top panels) and galaxy stellar mass (bottom panels), respectively. Both the star-forming (left panels, cyan shaded region) and passive (right panels, red shaded region) show high incidence of Lyα absorption. The width of the shaded regions represents 1σ uncertainty on f_C. The bins along x-axes were chosen to have approximately similar number of galaxies per bin.

Зависимости эквивалентной ширины Lyα от расстояния до центра и массы галактики

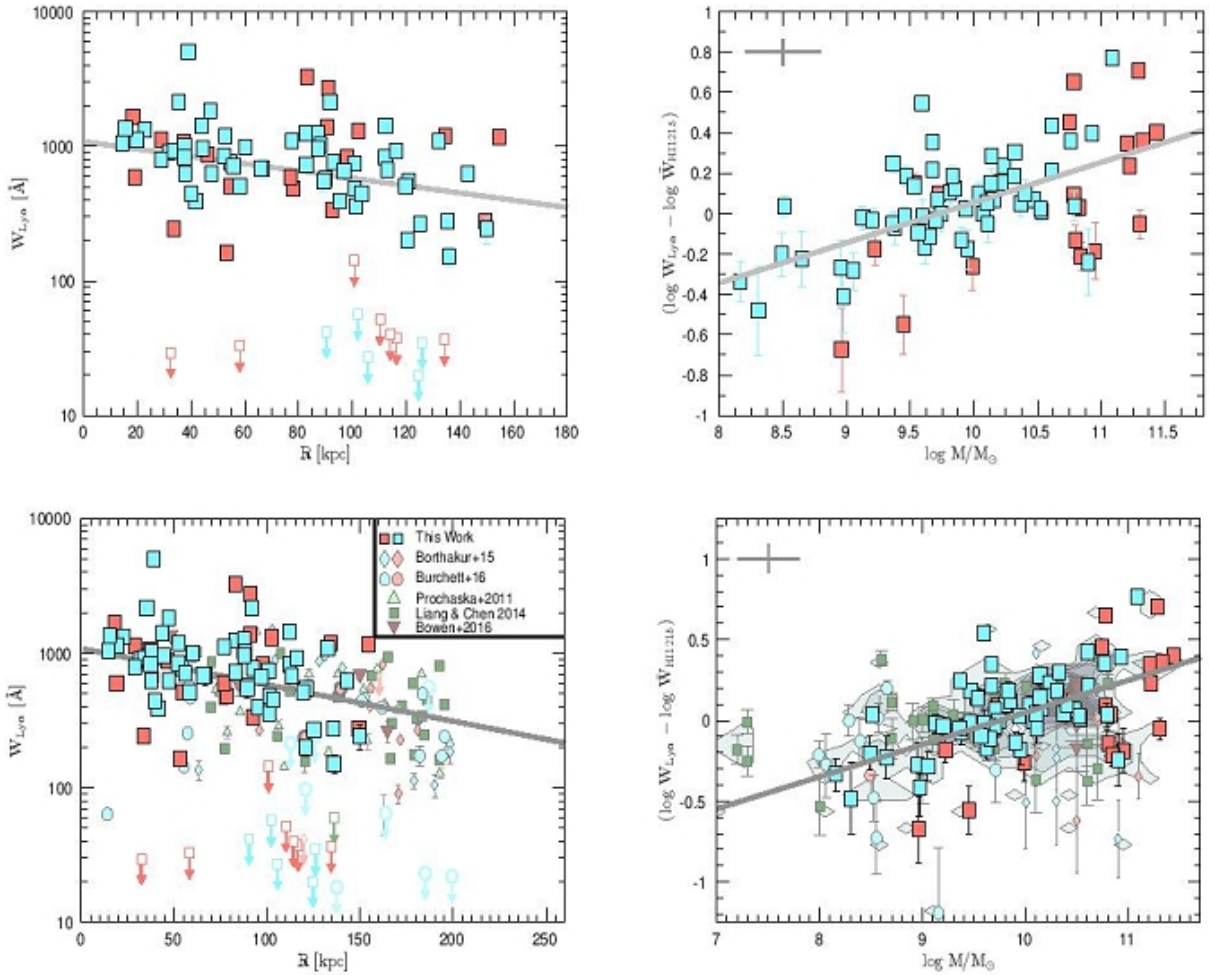

FIG. 2.— *Left Panels*: Lyα absorption radial profile from this work (top left), and archival data (bottom left), respectively. The solid gray line shows the best fit radial profile from equation 1. *Right Panels*: The $W_{Ly\alpha}$ absorption residuals as a function of stellar mass, showing strong correlation between the Lyα absorption strength and stellar mass for both the star-forming (blue squares) and passive (red squares) galaxies. The underlying contour on the bottom right panel traces the number density of galaxies in the plot. The gray crosses on right panels represent typical uncertainties associated with $W_{Ly\alpha}$ residual measurements and stellar mass estimates.

Фундаментальная плоскость!

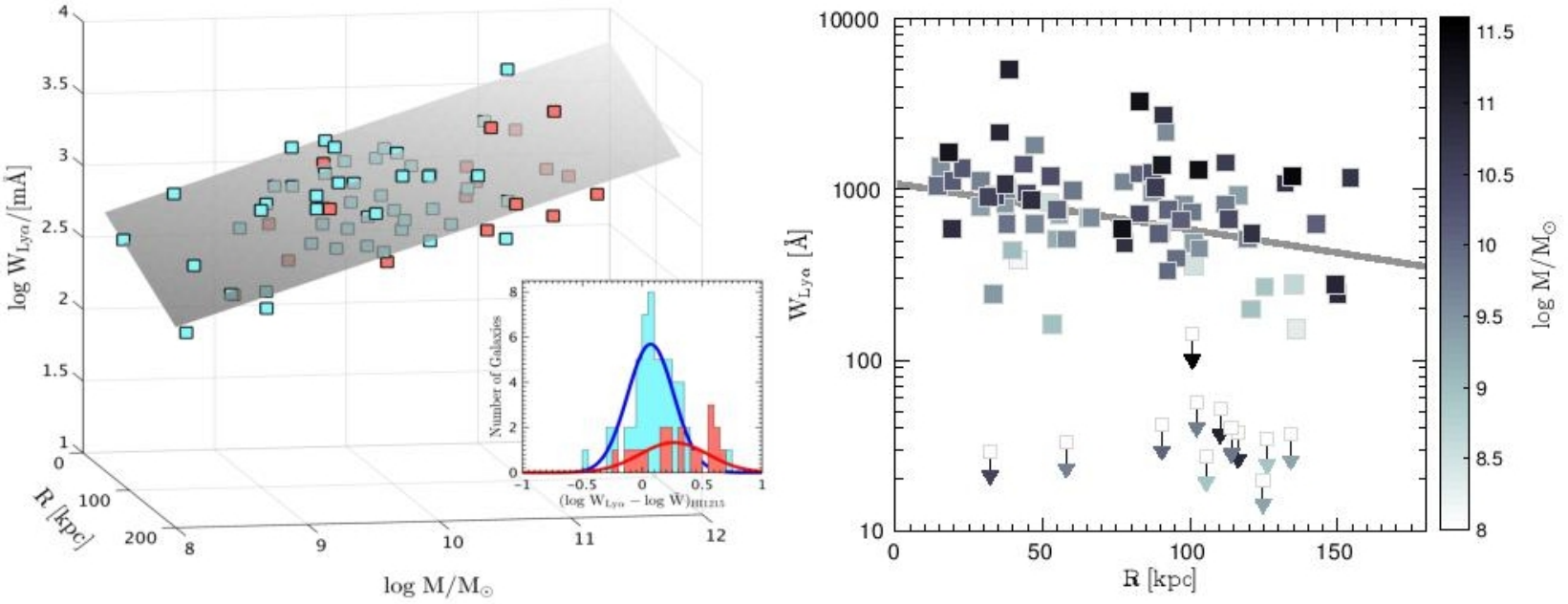

FIG. 3.— *Left Panel:* A surface fit showing the Lyα absorption within 160 kpc of the host galaxies across three decades of stellar mass. At a given stellar mass and impact parameter, the Lyα absorption strength can be predicted by the slope of this surface. The inset shows the residual equivalent widths of the fit for the whole sample. *Right Panel:* The radial profile of Lyα absorption for the same galaxies, color coded with their stellar mass. The higher mass galaxies typically segregate towards higher equivalent widths at all impact parameters.